International Journal of Thermophysics, Vol. 14, No. 4, 1993

Argon + Carbon Dioxide Gaseous Mixture Viscosities and Anisotropic Pair Potential Energy Functions[1]

I. N. Hunter,[2] G. Marsh,[3] G. P. Matthews,[4,5] and E. B. Smith[3]

Received December 31, 1992

The viscosities of pure gaseous carbon dioxide and argon + carbon dioxide mixtures have been measured with a capillary flow viscometer. The viscosities are relative to those of argon, in the temperature range 213 to 353 K, and considered accurate to ±0.7%. The pure-component viscosities agree closely with previous measurements. The mixture viscosities are used to calculate interaction viscosities and binary diffusion coefficients, which are compared with previous measurements. Interaction viscosities have been calculated, by use of the Mason–Monchick approximation, from the anisotropic pair potential energy functions for the unlike interaction proposed by Pack and his co-workers and by Hough and Howard. Comparison of these calculated interaction viscosities with those derived from our experiments and the higher-temperature measurements of Hobley, Matthews, and Townsend proves to be a powerful discriminant for the proposed anisotropic potential functions.

KEY WORDS: argon; carbon dioxide; mixtures; pair potential energy functions; viscosity.

1. INTRODUCTION

The transport properties of gases, in particular their viscosities, continue to be an important source of information in the study of intermolecular forces. Much attention has been focused on anisotropic interactions between atoms and molecules, such as the atom–quadrupole interaction of argon

[1] Paper dedicated to Professor Joseph Kestin.

[2] Shell UK Exploration and Production, Altens Farm Road, Nigg, Aberdeen AB9 2HY, United Kingdom.

[3] Physical Chemistry Laboratory, South Parks Road, Oxford OX1 3QZ, United Kingdom.

[4] Department of Environmental Sciences, University of Plymouth, Drake Circus, Plymouth, PL4 8AA, United Kingdom.

[5] To whom all correspondence should be addressed.

0195-928X/93/0700-0819$07.00/0

and carbon dioxide studied in this work. Several angle-dependent anisotropic pair potential energy functions have been proposed for the $Ar + CO_2$ system, most notably by Pack and co-workers [1–3] and Hough and Howard [4, 5]. Howard and co-workers have also studied interactions between atoms and dipolar molecules, such as $Ar + HCl$ and $Xe + HCl$ [6, 7], as well as the $Ar + OCS$ and $N_2 + CO_2$ interactions [8, 9].

The intermolecular interaction between two spherical molecules (or atoms) in the gas phase can be characterized in terms of a pair potential energy function $U(r)$ which describes the overall resultant (positive) repulsive energy between the molecules at small separations r, the resultant (negative) attractive energy at larger distances, and the asymptotic approach of the resultant attractive energy to zero at very large separations. Two characteristic features of this function are, first, the separation at which the interaction energy passes through zero, this distance being referred to as the collision diameter σ, and, second, the position of minimum interaction energy U, i.e. of greatest attraction. This position is referred to as the equilibrium separation r_m at which the interaction energy has a value $-\varepsilon$, where ε is termed the well depth. If $U(r)$ is known, the various transport properties of the system may be calculated by rigorous kinetic theory, which uses equations involving collision integrals, $\Omega^{(l,s)}$, which are integrals over the full range of energies, trajectories of collision, and orientations of the molecules during collisions. For a function $U_{12}(r)$ which applies to the cross interaction of two unlike molecules, the properties which are calculated are hypothetical ones arising only from collisions between unlike molecules, while real experimental properties arise from a combination of both like and unlike interactions. The hypothetical viscosity of this type is known as the interaction viscosity η_{12}, which to first order in the Chapman–Enskog formulation, is

$$\eta_{12} = \frac{5}{16}\left(\frac{m_{12}kT}{\pi}\right)^{1/2} \frac{1}{\sigma_{12}^2 \Omega_{12}^{(2,2)*}(T_{12}^*)} \tag{1}$$

Here k is the Boltzmann constant, T is the thermodynamic temperature, and the molar mass m_{12} of the hypothetical species is twice the reduced mass of the system, i.e., $2m_1m_2/(m_1+m_2)$. The reduced collision integral $\Omega_{12}^{(2,2)*}$ is a function of the reduced temperature $T_{12}^* = kT/\varepsilon_{12}$, where ε_{12} is the well depth of the unlike interaction.

In the case of mixtures of gaseous atoms or spherical molecules, the interaction viscosities can be "inverted" to yield an isotropic pair potential energy function [10]. For polyatomic systems, an effective isotropic potential function can be derived by inverting interaction viscosities, but its physical meaning is not clearly defined. Nevertheless, the forward calcula-

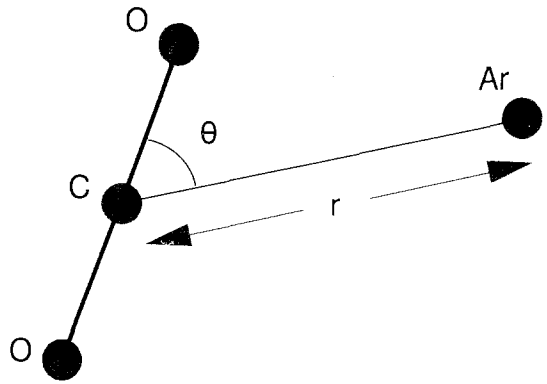

Fig. 1. The coordinates r and θ for the interaction of rigid, linear CO_2 with Ar.

tion, from anisotropic potential energy surfaces $U(r, \theta)$ to interaction viscosities, is useful. Most commonly the Mason–Monchick approximation [10], which is the classical equivalent of the "infinite order sudden" approximation, is employed. Within this approximation, the collision integrals $\Omega_{12}^{(l,s)*}$ are defined as equally weighted averages for each fixed orientation θ, so that

$$\Omega_{12}^{(l,s)*}(T^*) = \langle \Omega_{12}^{(l,s)*}(T^*, \theta) \rangle = \tfrac{1}{2} \int_{-1}^{+1} \Omega_{12}^{(l,s)*}(T^*, \theta)\, d(\cos\theta) \qquad (2)$$

In this work, we assume that the carbon dioxide molecule is a rigid, linear rotor, and θ and r are defined as shown in Fig. 1. It is also possible to calculate the interaction viscosities η_{12} of a system from the experimental measurements. The viscosities of both the pure components and at least one mixture are required. However, the calculation demands an estimate of ε_{12} to generate the ratio of reduced collision integrals $A_{12}^* = \Omega_{12}^{(1,2)*}/\Omega_{12}^{(1,1)*}$ [10]. Fortunately, A_{12}^* is insensitive to the shape of the potential function used to generate it.

2. EXPERIMENTS

Argon + carbon dioxide viscosities have been measured with two capillary flow gas viscometers. The pressure drop of the gas, and hence its rate of flow, is measured as it moves from a sample vessel, through a coiled capillary tube mounted in a cryostat, and then into a "back" vessel at a lower pressure. The two sets of apparatus have been described fully in previous publications [11, 12].

Both the argon and the carbon dioxide were 99.998% pure, with

major impurity nitrogen. Experiments were carried out on mixtures of mole fractions 0.25, 0.50, and 0.75, measured gravimetrically to within 0.1% mole fraction of the component of lowest composition in a particular mixture. The measurements were made at six temperatures in the temperature range 213 to 353 K, measured with a platinum resistance thermometer calibrated to an accuracy of 0.1 K. Various pressure regimes were used, absolute pressures being measured by means of a cathetometer accurate to 0.05 Torr. The experiments at 213 K were repeated on the more recently constructed viscometer. A consideration of the effects of possible random and systematic errors led to an estimated error in viscosity of $\pm 0.7\%$. This estimate was in accord with a check of accuracy in the form of measurements of the viscosity of pure carbon dioxide relative to that of argon.

Measurements of the pure-component viscosities and those of argon + carbon dioxide mixtures required corrections for the kinetic energy gained by the flowing gas, for gas imperfection, and for slip flow due to nonzero velocity at the walls of the capillary tube. A correction also arises from the increased resistance to flow due to the curvature of the helical capillary tube. This resistance is measured in terms of a dimensionless quantity call the Dean number, which increases with flow rate. Only runs with Dean numbers less than 6 were used. Under these conditions the correction for curved pipe flow is negligible.

Once the flow times are corrected as described, then it may be shown that for a particular temperature the viscosities η are related to the corrected flow times t^{corr} by the simple working equation

$$\frac{\eta_{\text{sample}}}{\eta_{\text{argon}}} = \frac{t^{\text{corr}}_{\text{sample}}}{t^{\text{corr}}_{\text{argon}}} \tag{3}$$

The corrected flow time ratios, i.e., the right-hand terms of Eq. (3), are shown in Tables I and II. The second columns show the mean pressure in the capillary tube during a particular run. Those measurements carried out with the newer apparatus are indicated with a superscript asterisk. To convert the relative viscosities to absolute values, argon standard viscosities must be used to supply the term η_{argon}. They were in the form

$$\ln(\eta_{\text{argon}}/\eta_0) = A \ln(T/T_0) + B/T + C/T^2 + D \tag{4}$$

where T_0 is 1 K, with coefficients as listed in Table III [13].

Also shown in Table III are the coefficients which provide the carbon dioxide viscosities recommended by Maitland and Smith [13]. All the carbon dioxide viscosities measured in this work were within $\pm 0.5\%$ of these values.

Table I. Measured Viscosities of Pure CO_2 and 75% CO_2 + 25% Ar

Temperature (K)	Mean pressure (mm Hg)	Pure CO_2 flow time ratio	Pure CO_2 viscosity (10^{-6} kg · m^{-1} · s^{-1})	Pure CO_2 mean viscosity (10^{-6} kg · m^{-1} · s^{-1})	75% CO_2 flow time ratio	75% CO_2 viscosity (10^{-6} kg · m^{-1} · s^{-1})	75% CO_2 mean viscosity (10^{-6} kg · m^{-1} · s^{-1})
213.15	156.9	0.79212	10.768	10.77	0.89723	12.197	12.20
	154.6	0.79089	10.752		0.89699	12.194	
	153.4	0.79292	10.779		0.89748	12.201	
213.15*	152.5	0.78788	10.711	10.73	0.89493	12.166	12.18
	148.6	0.78862	10.721		0.89498	12.167	
	145.1	0.79032	10.744		0.89706	12.195	
233.15	156.9	0.80155	11.734	11.74	0.91052	13.329	13.33
	154.6	0.80142	11.732		0.91033	13.326	
	153.4	0.80181	11.738		0.91118	13.339	
253.15	156.9	0.81751	12.790	12.79	0.92072	14.405	14.40
	154.6	0.81844	12.805		0.92143	14.416	
	153.4	0.81721	12.785		0.91990	14.392	
301.00	233.7	0.83736	15.003	15.02	0.94255	16.888	16.90
	231.4	0.83863	15.026		0.94320	16.900	
	229.7	0.83935	15.039		0.94401	16.914	
313.15	310.7	0.84558	15.616	15.62	0.94985	17.542	17.54
	308.2	0.84593	15.623		0.95008	17.546	
	306.5	0.84593	15.620		0.94977	17.540	
353.15	310.7	0.86511	17.492	17.48	0.96753	19.563	19.58
	308.2	0.86455	17.481		0.96807	19.574	
	306.5	0.86421	17.474		0.96904	19.593	

Table II. Measured Viscosities of 50% CO_2 + 50% Ar and 25% CO_2 + 75% Ar

Temperature (K)	Mean pressure (mm Hg)	50% CO_2 flow time ratio	50% CO_2 viscosity (10^{-6} kg·m^{-1}·s^{-1})	50% CO_2 mean viscosity (10^{-6} kg·m^{-1}·s^{-1})	25% CO_2 flow time ratio	25% CO_2 viscosity (10^{-6} kg·m^{-1}·s^{-1})	25% CO_2 mean viscosity (10^{-6} kg·m^{-1}·s^{-1})
213.15	156.9	1.0074	13.695	13.69	1.1244	15.285	15.31
	154.6	1.0064	13.681		1.1256	15.302	
	153.4	1.0067	13.685		1.1282	15.337	
213.15*	152.5	1.0042	13.652	13.68	1.1184	15.204	15.22
	148.6	1.0062	13.679		1.1199	15.224	
	145.1	1.0091	13.718		1.1205	15.232	
233.15	156.9	1.0184	14.909	14.93	1.1326	16.580	16.60
	154.6	1.0200	14.932		1.1346	16.609	
	153.4	1.0202	14.935		1.1343	16.605	
253.15	156.9	1.0268	16.065	16.07	1.1433	17.887	17.88
	154.6	1.0281	16.085		1.1436	17.892	
	153.4	1.0265	16.060		1.1410	17.851	
301.00	156.9	1.0497	18.808	18.83	1.1571	20.733	20.75
	154.6	1.0504	18.802		1.1594	20.773	
	153.4	1.0529	18.865		1.1584	20.755	
313.15	310.7	1.0571	19.522	19.54	1.1672	21.557	21.58
	308.2	1.0589	19.555		1.1691	21.591	
	306.5	1.0581	19.541		1.1685	21.580	
353.15	310.7	1.0725	21.686	21.69	1.1805	23.869	23.86
	308.2	1.0722	21.679		1.1782	23.823	
	306.5	1.0734	21.704		1.1811	23.881	

Table III. Coefficients of Eq. (3) for the Argon and Carbon Dioxide Standard Viscosities, for the Combined Interaction Viscosities η_{12} and Diffusion Coefficients D_{12}

	A	B (K)	C (K^2)	D	η_0 (10^{-6} kg·m^{-1}·s^{-1}) or $pD_{12,0}$(N·s^{-1})[a]
CO_2	0.52662	−97.589	2650.7	−2.6892	20.32
Ar	0.59077	−92.577	2990.4	−3.0755	22.28
η_{12}	0.35058	−252.56	14196.0	1.6409	0.1
D_{12}	1.42828	−206.035	11548.0	−9.48328	0.1

[a] p = pressure, N·m^{-2}.

Interaction viscosities η_{12} were then calculated from the mixture viscosities and the viscosities of the pure components. The omega integral ratios A^*_{12} required in these calculations were those of the argon BBMS potential function [14]. The well depth ε/k of 182 K used to calculate the reduced temperatures was that of Hobley et al. [15]. The resulting T^* and A^*_{12} values are shown in Table IV. Also shown are the calculated interaction viscosities at each temperature, calculated from the viscosities of the pure gases and those of the various mixtures shown at the head of each column. If both experiment and theory were perfectly accurate, identical η_{12} values for each mixture at a particular temperature would be obtained. In practice, the calculation of interaction viscosity is sensitive to errors in the pure component and mixture viscosities, and consequently the calculated η_{12} values are estimated to be accurate to $\pm 1.4\%$.

The interaction viscosities were combined with those of Hobley et al. [15] over the temperature range 301 to 521 K. A best-fitting curve of the

Table IV. Interaction Viscosities Calculated from the Experimental Mixture Viscosities of this Work

Temperature (K)	T^*	A^*_{12}	$\eta_{12}(10^{-6}$ kg·m^{-1}·s$^{-1})$		
			50% Ar + 50% CO_2	25% Ar + 75% CO_2	75% Ar + 25% CO_2
213.15	1.17	1.1084	14.104	14.117	14.283
213.15*	1.17	1.1084	14.096	14.127	13.996
233.15	1.28	1.1073	15.380	15.503	15.340
253.15	1.39	1.1062	16.348	16.531	16.581
301.00	1.65	1.1035	19.400	19.414	19.291
313.15	1.72	1.1029	20.134	20.108	20.181
353.15	1.94	1.1008	22.313	22.374	22.313

form of Eq. (4) was calculated for the combined data set, resulting in the coefficients listed in Table III. The deviations of the present interaction viscosities and those of other workers from this curve are shown in Fig. 2. The data are generally within $\pm 2\%$ of the curve, with the data of Kestin and Ro [16] exhibiting the most positive deviation.

$Ar + CO_2$ binary diffusion coefficients were calculated by means of the first-order relation [10]

$$D_{12} = \frac{3}{5} \frac{\eta_{12} A_{12}^* RT}{P m_{12}} \tag{5}$$

where P is the pressure and R the gas constant. Table III gives the coefficients for the best-fitting curve for these data combined with those of Hobley et al. Figure 3 shows that the diffusion coefficients calculated in this work lie within 1.2% of the fitting curve, within the expected experimental error of the interaction viscosities from which they are derived. The diffusion coefficients from this work and from Hobley et al. are calculated for each separate mixture, the latter having a relatively wide scatter. The experimental interaction viscosities of Kestin and Ro [16] give diffusion coefficients which are also very close to the fitted curve, deviating by not more than 0.5%. However Kestin and Ro's corresponding-states model [17] deviates from the fitting curve by more than 1%.

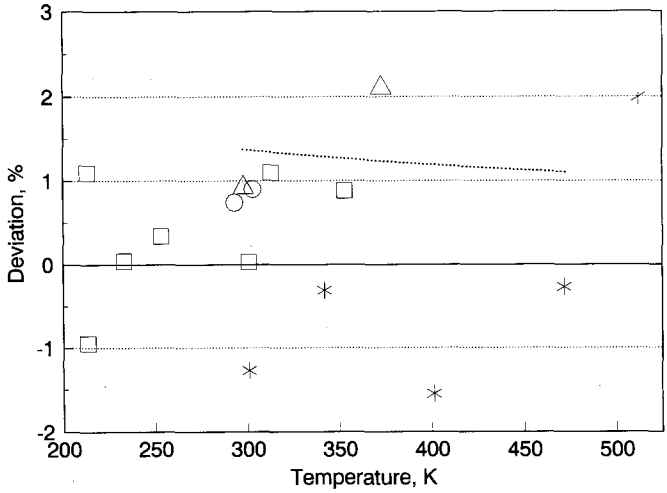

Fig. 2. Deviations of interaction viscosities η_{12} from the fitting curve of Table III. □, This work; ∗, Hobley et al. [15]; △, Kestin and Ro [16]; · · · · ·, Kestin and Ro [17]; ○, Kestin et al. [18].

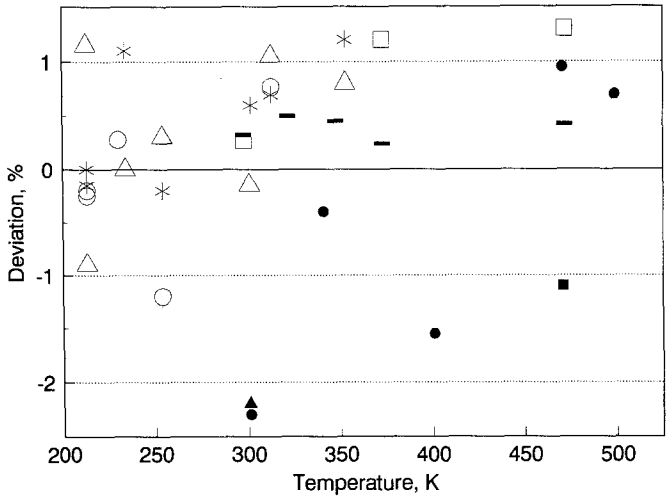

Fig. 3. Deviations of calculated binary diffusion coefficients D_{12} from the fitting curve of Table III. ∗, This work, 25% Ar (+75% CO_2); ○, this work, 50% Ar; △, this work, 75% Ar; ▲, Hobley et al., 25% Ar [15]; ●, Hobley et al., 50% Ar [15]; ■, Hobley et al., 75% Ar [15]; ▬, Kestin and Ro [16]; □, Kestin and Ro [17].

3. ANISOTROPIC PAIR POTENTIAL ENERGY FUNCTIONS

In this section we describe the various potential energy functions proposed for the Ar–CO_2 interaction by other workers, then calculate viscosities from them via the Mason–Monchick approximation.

3.1. The Potential Functions of Pack and Co-Workers

Pack and co-workers [1–3] have calculated various anisotropic potential energy surfaces $U(r, \theta)$ for the argon + carbon dioxide interaction. In this work we apply the Mason–Monchick approximation to a representative selection of three, referred to as Pack 1, Pack 2, and Pack 3. The Pack 1 surface [1] was calculated by means of the electron gas approximation at short range, of the form

$$\begin{aligned} U(r, \theta) &= E(r, \theta) - E(\infty, \text{any } \theta) \\ &= U_{\text{HF}}(r, \theta) + U_{\text{COR}}(r, \theta) \end{aligned} \tag{6}$$

and

$$V_{\text{HF}} = V_{\text{COUL}} + V_{\text{KIN}} + V_{\text{EXC}} \tag{7}$$

where E is the absolute potential energy of the molecule, and the subscripts refer to the Hartree Fock, correlation, coulomb, kinetic, and exchange contributions to the interaction energy. At long range, the surface was joined to a semiempirical van der Waals potential, incorporating theoretical C_6 and C_8 coefficients [19]. The potential parameters were adjusted so that there was good agreement with experimental second virial coefficients of Cottrell et al. [20] and Brewer [21], and there was reasonable agreement with high-energy scattering data. Various ways of joining the short- and long-range functions were presented, and our Pack 1 surface is that which gives the highest angular dependence of the well depth ε.

A second surface, Pack 2 [2], takes into account the rotational inelasticity in carbon dioxide. It gives good agreement with differential scattering cross sections. Again, various surfaces are described, and we employ the surface with highest angular dependence of ε.

To facilitate study of the damping of rainbow oscillations and diffraction oscillations in differential scattering cross sections, Pack [3] parameterized the previous surfaces in terms of an angle-dependent Lennard–Jones 12–6 potential function of the form

$$U(r, \theta) = \varepsilon(\theta)\{[r_m(\theta)/r]^{12} - 2[r_m(\theta)/r]^6\} \tag{8}$$

with

$$\varepsilon(\theta) = \bar{\varepsilon}[1 + aP_2(\cos\theta)] \tag{9}$$

and

$$r_m(\theta) = \bar{r}_m[1 + bP_2(\cos\theta)] \tag{10}$$

P_2 being the second Legendre polynomial. For $Ar + CO_2$, Pack used $\bar{\varepsilon} = 200$ K and $\bar{r}_m = 0.388$ nm. Surfaces with various a and b values were presented, of which our Pack 3 surface has $a = 0.0$ and $b = 0.2$.

We have determined the Mason–Monchick angular averages of the Pack 1, 2, and 3 surfaces. The calculations used the seven positive pivots of a 14-point Gauss Legendre quadrature which yields collision integrals $\Omega_{12}^{(2,2)*}$ with an estimated uncertainty of no more than $\pm 0.2\%$. Figure 4 shows cross sections of the Pack 1, Pack 2, and Pack 3 potential energy surfaces at two of the seven pivots used in our calculations, these being at $\theta = 88.5$ and $13.0°$. Interaction viscosities derived from the collision integrals are listed in Table V.

The interaction viscosities calculated from the Pack 1 surface are within 0.25% of similar calculations by Maitland et al. [22] as modified by Vesovic [23]. The corresponding diffusion coefficients D_{12} of Maitland

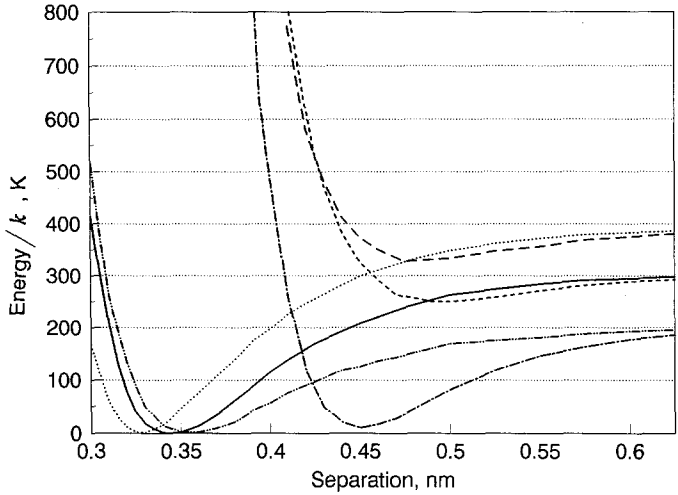

Fig. 4. Cross sections through potential energy surfaces of Pack and co-workers at $\theta = 88.5$ and 13°. Pack 1: ——, 88.5°; ------, 13° [1]. Pack 2: ····· ····· ·····, 88.5°; – – –, 13° [2]. Pack 3: – · – · –, 88.5°; – · – · –, 13° [3].

et al. agree well with the experimentally based fitting curve of Table III, deviating by no more than 0.6%.

The deviation of the calculated viscosities about a fitted curve of experimental viscosities of this work and that of Hobley et al. [15] is shown in Fig. 5. The Pack 2 potential energy surface generates viscosities within 3% of the experimentally based interaction viscosities, whereas Pack 1 and Pack 3 generate viscosities up to 6% too low.

Table V. Interaction Viscosities η_{12} Calculated from the Potential Energy Surfaces of Pack and Co-Workers [1–3]

Temperature (K)	Pack 1 [1] (10^{-6} kg·m^{-1}·s^{-1})	Pack 2 [2] (10^{-6} kg·m^{-1}·s^{-1})	Pack 3 [3] (10^{-6} kg·m^{-1}·s^{-1})
200.0	13.30	13.25	12.66
300.0	18.82	18.96	18.35
400.0	23.67	24.14	23.48
500.0	28.09	28.86	28.12
600.0	32.12	33.20	32.36
700.0	35.87	37.24	36.30
800.0	39.41	41.06	39.99
900.0	42.78	44.70	43.49
1000.0	46.03	48.19	46.83

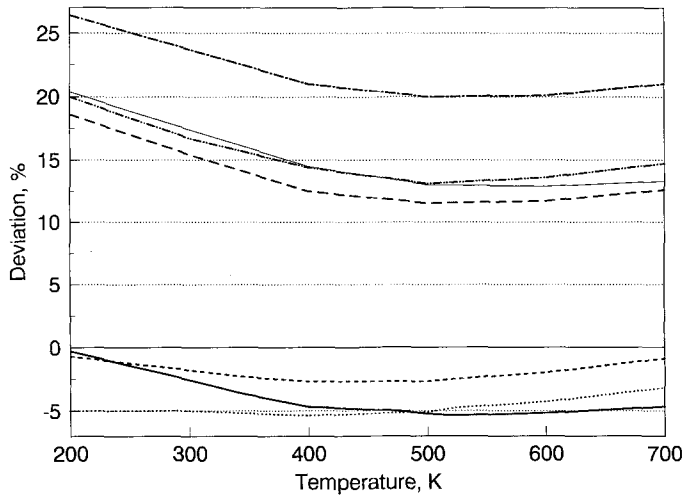

Fig. 5. Deviations of calculated interaction viscosities from the experimental fitting curve of Table III. ———, Pack 1 [1]; ------, Pack 2 [2]; · · · · · · · · · · · ·, Pack 3 [3]. Hough and Howard [4, 5]: ——, A3; – · · – · · –, A3-M; – · – · –, AD; ——, AD-M.

3.2. The Potential Functions of Hough and Howard

The latest angle-dependent potential energy surfaces for the $Ar + CO_2$ system were reported by Hough and Howard [4, 5]. The potentials of Hough and Howard were obtained by a simultaneous least-squares fit to molecular-beam electric resonance spectra, mixed second virial coefficients, and mean square torque measurements. Their potential function was expressed as an angle-dependent parameterisation of the Maitland–Smith $n(r^*)$–6 function:

$$U(r, \theta) = [\varepsilon(\theta)/\{n(\theta) - 6\}][6x(\theta)^{-n(\theta)} - n(\theta)\, x(\theta)^{-6}] \tag{11}$$

with

$$n(\theta) = m(\theta) + \gamma[x(\theta) - 1] \tag{12}$$

and

$$x(\theta) = r/r_m(\theta) \tag{13}$$

Here $m(\theta)$ is related to the radial curvature at the radial minimum and is a shape skewing parameter. For noble gases a value of $m = 13$ is usually applied, though this parameter has been varied in two of the Hough and

Howard potentials. The value of γ is less crucial, and they used a value of 9 in all their proposed potential functions. The parameters $\varepsilon(\theta)$ and $r_m(\theta)$ were expressed as sums of even Legendre polynomials, in a similar style to the Pack 3 potential surface parameterisation.

Figure 6 shows cross sections through the 3A potential energy surface for the three angle parameterization with the value of m fixed at 13 and the potential of the linear geometry fixed with $r_m(\theta)$ at between 0.49 and 0.50 nm. The variation of $r_m(\theta)$ is relatively similar to those of Pack, but the variation in well depths is some way between the two extremes of the Pack 2 and 3 potentials, having well depths between 201 and 56 K.

The second potential energy surface described by Hough and Howard was the 3A-M, which was the 3A potential with the repulsive parameter m included in the optimization. This gives a potential surface which is very similar to 3A, having slightly shallower well depths as θ approaches zero. However, the main difference is in the linear configuration, due to the fact that r_m is not fixed.

The third potential surface described is the angle-dependent AD potential, with m fixed at 13. A cross section at $\theta = 13°$ is shown in Fig. 6. A problem pointed out by Hough and Howard for this surface was that the Legendre polynomial P_4 dominates the P_2 term near 90°. This causes the radial distance to decreases on either side of the potential minimum, which is unrealistic. The final potential quoted by Hough and Howard was the

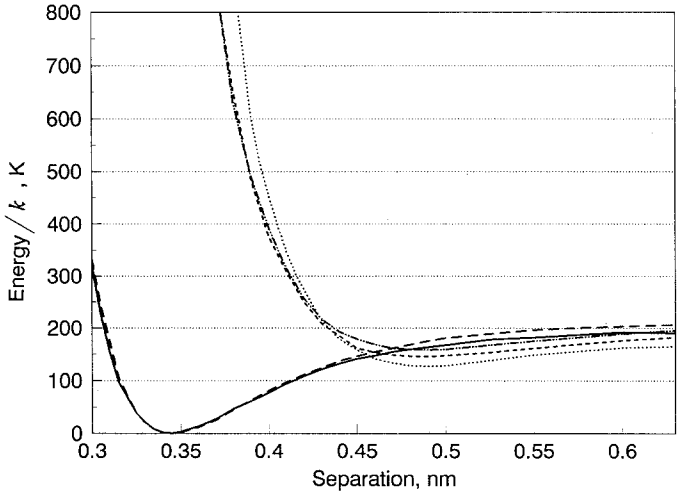

Fig. 6. Cross sections through potential energy surfaces of Hough and Howard [4, 5] at $\theta = 88.5$ and 13°. ——, 3A, 88.5°; ------, 3A, 13.0°; · · · · · · · · · · · ·, AD, 13.0°; – – –, AD-M, 88.5°; – · – · –, AD-M, 13.0°.

Table VI. Interaction Viscosities η_{12} Calculated from the Potential Energy Surfaces of Hough and Howard [4, 5]

Temperature (K)	3A (10^{-6} kg·m^{-1}·s^{-1})	3A-M (10^{-6} kg·m^{-1}·s^{-1})	AD (10^{-6} kg·m^{-1}·s^{-1})	AD-M (10^{-6} kg·m^{-1}·s^{-1})
200.0	15.85	16.03	16.88	16.10
300.0	22.33	22.59	23.91	22.72
400.0	28.00	28.38	30.07	28.47
500.0	33.13	33.65	35.61	33.60
600.0	37.89	38.55	40.73	38.30
700.0	42.36	43.16	45.52	42.68
800.0	46.62	47.55	50.08	46.82
900.0	50.67	51.74	54.45	50.76
1000.0	54.62	55.77	58.65	54.56

AD-M, which is the same as the AD surface with m included as a potential variable (Fig. 6). The AD and AD-M cross sections at 88.5° are similar on the scale of Fig. 6.

Table VI lists the viscosity values calculated from the Hough and Howard potentials using the Mason–Monchick approximation. They are up to 27% higher than the experimentally based interaction viscosities, as shown in Fig. 5.

4. DISCUSSION

The calculation of interaction viscosities from potential energy surfaces by means of the Mason–Monchick approximation, and subsequent comparison with experimentally based values, has been shown to provide a powerful test of the accuracy of the surfaces. The Pack 2 potential energy surface [2] reproduces the interaction viscosities with reasonable accuracy. This surface is Pack's own optimization of the Pack 1 surface, whereas the Pack 3 is merely a trial parameterization. The optimum fit of the Pack 2 surface therefore agrees with Pack's own findings based on entirely different experimental properties. The surfaces of Howard and co-workers give very much greater deviations. The Mason–Monchick approximation is considered accurate to a few percent, and the errors must arise from the quality of the potential energy surfaces. The discrepancies may occur because of the use of insufficiently flexible parameterization or from errors in the data on which the potentials are based.

ACKNOWLEDGMENTS

I. N. Hunter acknowledges receipt of an SERC CASE studentship with the National Engineering Laboratory. The authors than Dr. A. Scott of that institution for his interest and support.

REFERENCES

1. G. A. Parker, R. L. Snow, and R. T. Pack, *J. Chem. Phys.* **64**:1668 (1976).
2. R. K. Preston and R. T. Pack, *J. Chem. Phys.* **66**:2480 (1977).
3. R. T. Pack, *Chem. Phys. Lett.* **55**:197 (1978).
4. A. M. Hough and B. J. Howard, *J. Chem. Soc. Faraday Trans. 2* **83**:173 (1987).
5. A. M. Hough and B. J. Howard, *J. Chem. Soc. Faraday Trans. 2* **83**:191 (1987).
6. J. M. Hutson and B. J. Howard, *Mol. Phys.* **45**:769 (1982).
7. J. M. Hutson, *J. Chem. Phys.* **89**:4550 (1988).
8. G. D. Hayman, J. Hodje, B. J. Howard, J. S. Muenter, and T. R. Dyke, *J. Mol. Spectrosc.* **133**:423 (1989).
9. M. A. Walsh, T. R. Dyke, and B. J. Howard, *J. Mol. Struct.* **189**:111 (1988).
10. G. C. Maitland, M. Rigby, E. B. Smith, and W. A. Wakeham, *Intermolecular Forces* (Oxford University Press, Oxford, 1981).
11. A. G. Clarke and E. B. Smith, *J. Chem. Phys.* **48**:1988 (1968).
12. I. N. Hunter, G. P. Matthews and E. B. Smith, *J. Chem. Soc. Faraday Trans.* **87**:2161 (1991).
13. G. C. Maitland and E. B. Smith, *J. Chem. Eng. Data* **17**:150 (1972).
14. G. C. Maitland and E. B. Smith, *Mol. Phys.* **22**:861 (1971).
15. A. Hobley, G. P. Matthews, and A. Townsend, *Int. J. Thermophys.* **10**:1165 (1989).
16. J. Kestin and S. T. Ro, *Ber. Bunsen-Gesellschaft Phys. Chem.* **78**:20 (1974).
17. J. Kestin and S. T. Ro, *Ber. Bunsen-Gesellschaft Phys. Chem.* **80**:619 (1976).
18. J. Kestin, Y. Kobayashi, and R. T. Wood, *Physica* **32**:1065 (1966).
19. R. T. Pack, *J. Chem. Phys.* **64**:1659 (1976).
20. T. L. Cotterell, R. A. Hamilton, and R. P. Taubinger, *Trans. Faraday Soc.* **52**:1310 (1956).
21. J. Brewer, Tech. Report, AD 663448 (1967).
22. G. C. Maitland, M. Mustafa, V. Vesovic, and W. A. Wakeham, *Mol. Phys.* **57**:1015 (1986).
23. V. Vesovic, personal communication.